Atmos. Chem. Phys., 9, 1735–1746, 2009
www.atmos-chem-phys.net/9/1735/2009/

Atmospheric Chemistry and Physics

Stratospheric $BrONO_2$ observed by MIPAS

M. Höpfner[1], J. Orphal[2], T. von Clarmann[1], G. Stiller[1], and H. Fischer[1]

[1]Institut für Meteorologie und Klimaforschung, Forschungszentrum Karlsruhe, Germany
[2]Laboratoire Interuniversitaire des Systèmes Atmosphériques, CNRS UMR 7583, Université de Paris-Est, Créteil, France

Received: 7 August 2008 – Published in Atmos. Chem. Phys. Discuss.: 19 November 2008
Revised: 19 February 2009 – Accepted: 26 February 2009 – Published: 6 March 2009

Abstract. The first measurements of stratospheric bromine nitrate ($BrONO_2$) are reported. Bromine nitrate has been clearly identified in atmospheric infrared emission spectra recorded with the Michelson Interferometer for Passive Atmospheric Sounding (MIPAS) aboard the European Envisat satellite, and stratospheric concentration profiles have been determined for different conditions (day and night, different latitudes). The $BrONO_2$ concentrations show strong day/night variations, with much lower concentrations during the day. Maximum volume mixing ratios observed during night are 20 to 25 pptv. The observed concentration profiles are in agreement with estimations from photochemical models and show that the current understanding of stratospheric bromine chemistry is generally correct.

1 Introduction

Bromine nitrate, $BrONO_2$, is an important species in stratospheric bromine chemistry (Spencer and Rowland, 1978; Lary, 1996; Daniel et al., 1999) and it is closely linked to the chemical cycles of stratospheric ozone depletion (Daniel et al., 1999; Salawitch et al., 2005). In particular it is the most important reservoir species for inorganic stratospheric bromine. During the day, $BrONO_2$ is photolysed within a few minutes (Burkholder et al., 1995; Deters et al., 1998; Soller et al., 2002), but at the same time it is also produced continuously by the termolecular reaction between BrO, NO_2 and another collision partner, leading to quasi stationary concentrations that are mainly determined by the actinic flux, by the BrO and the NO_2 concentrations and by the air density (Lary, 1996). $BrONO_2$ can also be destroyed by heterogeneous reactions with H_2O on stratospheric aerosol forming HOBr and HNO_3 (Hanson et al., 1996; Lary et al., 1996; Tie and Brasseur, 1996), and by the reaction of $BrONO_2$ with O atoms that has been proposed as additional sink for bromine nitrate (Soller et al., 2001).

Until now, the only inorganic bromine species that has been measured extensively in the stratosphere is BrO, using either its electronic bands in the near ultraviolet (Fish et al., 1995; Aliwell et al., 1997; Harder et al., 2000; Pundt et al., 2002; Sinnhuber et al., 2005; Sheode et al., 2006; Sioris et al., 2006), its rotational lines in the microwave region (Kovalenko et al., 2007), or in-situ by resonance fluorescence spectroscopy (Avallone and Toohey, 2001). There are also some measurements of HBr and HOBr in the far-infrared region (Johnson et al., 1995; Carlotti et al., 1995; Nolt et al., 1997), however the concentrations of HBr and HOBr are generally much lower than those of BrO and $BrONO_2$, and for HOBr only an upper concentration limit was determined.

From these observations, together with measurements of organic bromine species and with photochemical models, the total inorganic bromine (Br_y = Br + 2×Br_2 + BrO + HBr + HOBr + $BrONO_2$ + BrCl) in the stratosphere and its partitioning can be derived (e.g. Fish et al., 1997; Harder et al., 2000; Pfeilsticker et al., 2000; Sinnhuber et al., 2002). The range of total inorganic bromine is estimated to 18–25 pptv (WMO, 2007). Recently, a slow decline (about 1% per year in the 2001–2005 period) of the total stratospheric bromine was reported based on BrO observations (Dorf et al., 2006; Hendrick et al., 2008). $BrONO_2$ concentrations depend strongly on the actinic flux, on available NO_2, and on aerosols like polar stratospheric clouds. It is estimated that $BrONO_2$ contributes a major part to the partitioning of Br_y during night (although in the lower stratosphere, as a product of heterogeneous chemistry, HOBr can also be an important night-time reservoir of active bromine) while during day its concentration can vary strongly.

Correspondence to: M. Höpfner
(michael.hoepfner@imk.fzk.de)

Published by Copernicus Publications on behalf of the European Geosciences Union.

In this context, measurements of stratospheric bromine nitrate are interesting to validate photochemical models and, thus, the current understanding of stratospheric bromine chemistry. Such measurements also provide an additional independent set of observations that would be useful as input for model calculations concerning the inorganic bromine budget and the bromine partitioning in the stratosphere.

In this paper we present the first detection of $BrONO_2$ in the stratosphere by use of MIPAS/Envisat measurements, and discuss the results in the context of previous studies, in particular concerning stratospheric BrO and the total inorganic bromine.

2 MIPAS

The MIPAS instrument is a Fourier transform spectrometer sounding the mid-infrared emission of the atmospheric trace gases between 685 and 2410 cm^{-1} (14.6–4.15 µm) in limb geometry from the sun-synchronous polar orbiting satellite Envisat (Fischer et al., 2008). Due to its ability to perform global observations independently of sunlight MIPAS is able to measure during day and night (including polar night) and can thus provide measurements of stratospheric $BrONO_2$ and its diurnal variation. Such measurements of the diurnal variation of $BrONO_2$ are particularly interesting since for most conditions, higher concentrations are expected during the night, as also observed for chlorine nitrate (Johnson et al., 1996), and they also provide an additional opportunity to compare the results with photochemical models.

For the present investigation we have used MIPAS nominal mode measurements taken in September 2002 and 2003 where the maximum optical path difference of the interferometer was 20 cm resulting in a spectral resolution (FWHM) of 0.048 cm^{-1} after apodisation with the Norton-Beer "strong" function (Norton and Beer, 1976). The field-of-view of the instrument at the tangent points is about 3 km in the vertical and 30 km in the horizontal. Each limb scan consisted of 17 spectra with nominal tangent altitudes of 6, 9, 12,..., 39, 42, 47, 52, 60, and 68 km. About 1000 limb scans were recorded during one day with an along track sampling of approximately 550 km. The raw signals were processed by the European Space Agency (ESA) to produce calibrated geolocated limb emission spectra, labelled level 1b data (Nett et al., 1999). For this study, level 1b data of version 4.61/62 have been used.

3 Data analysis and results

3.1 Retrieval strategy for $BrONO_2$

To retrieve $BrONO_2$ from MIPAS observations the spectral range of the ν_3 fundamental band around 803 cm^{-1} has been chosen using the spectroscopic dataset by Orphal et al. (2008) adapted for use at stratospheric temperatures as described in Sect. 3.4.1 below. Figure 1 shows an example of the contributing spectral signatures of various trace gases over the range of the $BrONO_2$ ν_3-band for a tangent altitude of 21 km. By far the most intense lines are those by CO_2 and O_3 with radiance contributions of more than 1000 $nW/(cm^2\,sr\,cm^{-1})$ directly followed by a few H_2O lines with radiances of up to 800 $nW/(cm^2\,sr\,cm^{-1})$. Trace gases with radiance signatures between about 100 and 300 $nW/(cm^2\,sr\,cm^{-1})$ are $ClONO_2$, NO_2, CFC−22, and HNO_4 and those between 1 and 30 $nW/(cm^2\,sr\,cm^{-1})$ are $BrONO_2$, COF_2, HNO_3, ClO (during day, increasing at higher altitudes), CCl_4, CFC−113, and PAN.

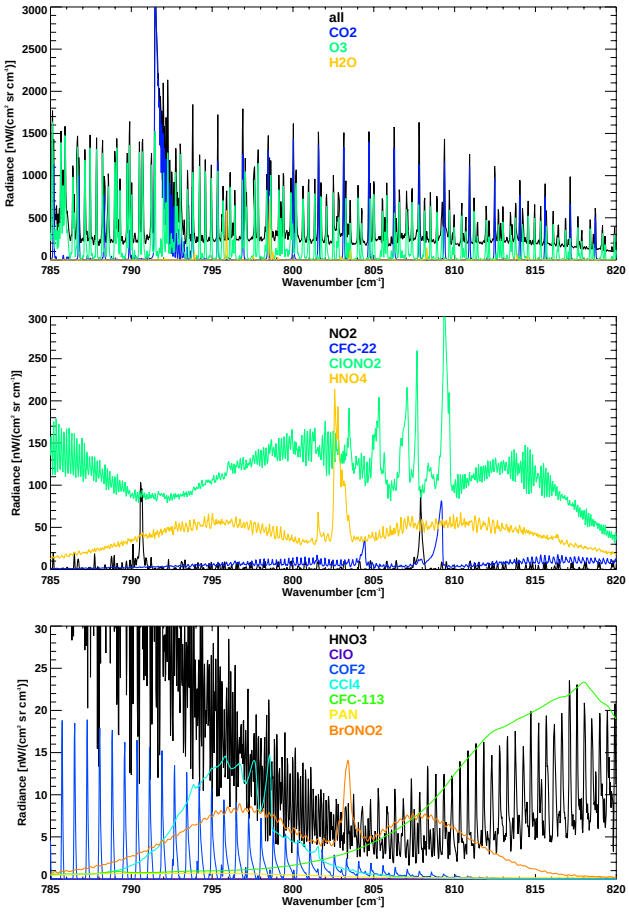

Fig. 1. Contributing trace gas signatures within the spectral range used for retrieval of BrONO2. The contributions are shown as radiances of each gas calculated independently of the other species. Calculations were made for a tangent altitude of 21 km using mid-latitude night standard vmr-profiles (Remedios et al., 2007) and using the retrieved concentration of $BrONO_2$ from the 15° N–40° N night range (see Table 1 and Fig. 2). Mind that from top to bottom the y-axis is zoomed.

Since the spectral noise of single MIPAS measurements is about 20 $nW/(cm^2\,sr\,cm^{-1})$ in the relevant spectral range,

Table 1. Selected time periods, latitude ranges, day (d) and night (n), in (i) and out (o) vortex conditions for which averaged spectra have been calculated. In/out vortex conditions are only relevant for the latitude range 90° S–40° S. The number of averaged single spectra, the estimated noise of the mean spectra, the mean latitudes and the mean solar zenith angles are given.

	Number of averaged spectra	Mean spectral noise[a]	Mean latitude	Mean solar zenith angle [°]
1–20 Sep 2002:				
90–40° S, d, i	1026	0.44	74.7° S	81.9
90–40° S, n, i	852	0.48	72.0° S	111.7
90–40° S, d, o	502	0.62	51.1° S	60.8
90–40° S, n, o	456	0.65	50.8° S	129.6
40–15° S, d, o	750	0.51	28.1° S	42.3
40–15° S, n, o	740	0.51	26.9° S	147.8
15° S–15° N, d, o	1265	0.39	1.4° S	28.8
15° S–15° N, n, o	952	0.45	1.5° S	153.8
15–40° N, d, o	1060	0.43	26.1° N	33.6
15–40° N, n, o	1230	0.40	28.9° N	138.6
40–65° N, d, o	1067	0.43	50.9° N	51.3
40–65° N, n, o	1041	0.43	56.1° N	115.9
65–90° N, d, o	1625	0.35	78.7° N	77.9
65–90° N, n, o	335	0.76	72.6° N	102.0
1–30 Sep 2003:				
90–40° S, d, i	1913	0.32	74.3° S	79.5
90–40° S, n, i	1434	0.37	70.5° S	111.5
90–40° S, d, o	688	0.53	48.2° S	56.3
90–40° S, n, o	623	0.56	47.5° S	130.5
40–15° S, d, o	1459	0.37	28.5° S	40.9
40–15° S, n, o	1396	0.37	27.6° S	146.2
15° S–15° N, d, o	1939	0.32	1.4° S	28.2
15° S–15° N, n, o	1686	0.34	0.5° N	153.6
15–40° N, d, o	1614	0.35	26.1° N	34.7
15–40° N, n, o	1727	0.34	30.1° N	139.6
40–65° N, d, o	1610	0.35	50.9° N	52.9
40–65° N, n, o	1596	0.35	56.1° N	117.8
65–90° N, d, o	2304	0.29	78.6° N	78.8
65–90° N, n, o	674	0.54	74.1° N	103.0

[a] Units: $[\mathrm{nW/(cm^2\,sr\,cm^{-1})}]$

it exceeds the maximum signal of $BrONO_2$ by a factor of 2 and more. Thus, the strategy adopted in this study for an unambiguous identification of stratospheric $BrONO_2$ is to use average MIPAS spectra over the time period of about one month for selected latitude bands, in- and out-vortex air-masses and day/night conditions. Additionally, to obtain independent datasets of different years we selected MIPAS observations from September 2002 and 2003. For averaging we selected only spectra which were not influenced by tropospheric or polar stratospheric clouds. For that purpose the cloud-index (CI) method by Spang et al. (2004) has been used applying a strict limit of CI=4.5 which means that even spectra affected by optically very thin polar stratospheric clouds are sorted out. Detailed information about the selection is given in Table 1: the typical reduction of the noise gained by averaging the spectra is about a factor of 50.

Due to a problem in the offset-calibration of the ESA-level 1b processing chain (A. Kleinert, personal communication) the averaged spectra had to be corrected before being used in the retrieval. Contrary to Stiller et al. (2008) who corrected the retrieved trace gas distributions, we have corrected the spectral radiances prior to the retrieval. The correction procedure is based on the fact that in the ESA processing the spectrally low-resolved deep space spectrum used for offset calibration has not been updated each fourth limb-scan, as intended, but instead a reference offset which was updated only once a week has been used. In this work, for correction of the average spectra we have subtracted a residual offset

spectrum. This offset spectrum has been determined from the uncorrected average spectra of the highest tangent altitude (about 68 km) from which remaining small CO_2 signatures have been removed by fit of a simulated CO_2 spectrum.

Beside the spectral noise, the influence of the interfering species is the main problem in determination of $BrONO_2$ from MIPAS measurements. To obtain a best possible fit of the simulations to the measured spectra we simultaneously retrieve all trace gases mentioned above, with the exception of CO_2, which, due to its known atmospheric concentration, was used to retrieve temperature profiles. Additionally, in order to account for instrumental artefacts, a height-independent tangent altitude offset, a spectral shift and a spectrally constant radiance contribution has been determined. Atmospheric and instrumental parameters are combined in the vector $\boldsymbol{x}$, which is determined in a Newtonian iteration process (Rodgers, 2000; von Clarmann et al., 2003):

$$\boldsymbol{x}_{i+1} = \boldsymbol{x}_i + (\mathbf{K}^T \mathbf{S}_y^{-1} \mathbf{K} + \mathbf{R})^{-1} \times \left[\mathbf{K}^T \mathbf{S}_y^{-1} (\boldsymbol{y}_{\text{meas}} - \boldsymbol{y}(\boldsymbol{x}_i)) - \mathbf{R}(\boldsymbol{x}_i - \boldsymbol{x}_a) \right]. \quad (1)$$

$\boldsymbol{y}_{\text{meas}}$ is the vector of selected measured spectral radiances of all tangent altitudes under investigation, and $\mathbf{S}_y$ is the related noise covariance matrix. $\boldsymbol{y}(\boldsymbol{x}_i)$ contains the spectral radiances calculated with the radiative transfer model KOPRA (Stiller, 2000) using the best guess atmospheric state parameters $\boldsymbol{x}_i$ of iteration number i. $\mathbf{K}$ is the Jacobian matrix, i.e. the partial derivatives $\partial \boldsymbol{y}(\boldsymbol{x}_i)/\partial \boldsymbol{x}_i$ calculated also with the radiative transfer model. $\mathbf{R}$ is the regularization matrix and $\boldsymbol{x}_a$ the a-priori information.

We have chosen the spectral interval from 801–820 cm^{-1} for the following reasons: (a) to avoid the CO_2 Q-branch at around 791 cm^{-1} for which very exact modelling of line-mixing effects would have been needed, (b) to exclude some of the O_3 lines below 800 cm^{-1} which cause – presumably due to inconsistent spectroscopic data – systematic spectral residuals, and (c) to minimize the influence of the simultaneously fitted gases CCl_4 and PAN. This reduced wavenumber range still contains enough information to obtain sufficiently small errors due to spectral noise in combination with a good vertical resolution.

The retrieval was performed on a 1 km grid using a first-order smoothing constraint $\mathbf{R}=\gamma \mathbf{L}^T \mathbf{L}$ with the altitude-independent but species-dependent regularisation parameters γ. $\mathbf{L}$ is a first order finite differences operator (Tikhonov, 1963). It is important to emphasize that for the target species of the present study, $BrONO_2$, the initial guess and the a-priori profiles, $\boldsymbol{x}_0$ and $\boldsymbol{x}_a$, have been set equal to zero, while for all other trace gases climatological values have been used. The initial guess and a-priori values of temperature have been determined as the mean profiles from the ECMWF analysis at the location and time of the single MIPAS measurements. The regularization strength was chosen such to avoid oscillatory structures in the retrieved profiles of all atmospheric parameters.

3.2 Results

Figure 2 shows the retrieved $BrONO_2$ profiles between 20 and 40 km altitude for the various sets of averaged spectra belonging to different years, latitude bands and in/out vortex conditions (Table 1). Estimated errors indicated in the plots are those due to spectral noise (bars) and the combination of spectral noise and systematic errors (dotted). The trace of the averaging kernel matrix reveals about four degrees of freedom of the retrieved profiles between 20 and 40 km altitude. The vertical resolution derived from the reciprocal of the averaging kernel diagonal values (Rodgers, 2000) ranges from around 3–5 km at lower to 6–10 km at higher altitudes.

In each plot, black curves indicate MIPAS nighttime observations while daytime measurements are plotted in red with the mean solar zenith angle given in Table 1. The fact that $BrONO_2$ vmr values obtained during night are always larger than those during day is in agreement with its photolytic destruction during sunlit conditions. Additionally, there is a general consistency of the results between the two years with maximum nighttime values of $BrONO_2$ between 20.8 and 24.5 pptv at altitudes of 25–31 km. The altitude of the daytime maximum is lower at high latitudes (23–24 km) compared to equatorial regions (27–29 km). The highest daytime values (12.4 and 13.4 pptv) are found at 65–90° N at 23 km altitude during both years. The maximum daytime volume mixing ratios at all other latitudes range between 5.6 and 8.4 pptv.

Small negative values are sometimes obtained in mid-latitude daytime profiles in 2003 but are mostly within the estimated total error bars. Only the equatorial daytime values above 33 km altitude reach negative (−4 pptv) values where the maximum total errors miss zero by 1–2 pptv. This indicates an effect of systematic nature affecting those profiles which might be due to errors caused by retrievals from mean spectra becoming the dominant error contribution at those altitudes for daytime retrievals as shown in Fig. 5 (called "nlin") and discussed in Sect. 3.4 below. This suggests clearly that daytime $BrONO_2$ concentrations above about 30–35 km are in general too low to be detected.

3.3 Spectral evidence for $BrONO_2$

Beyond the plausible and coherent $BrONO_2$ volume mixing ratio profiles obtained from the MIPAS retrievals including their day-night variation and the comparison between two different years, we now demonstrate its detection in the spectral domain.

In Fig. 3 the residual spectra resulting from the MIPAS $BrONO_2$ retrieval (i.e. the difference between measurement and simulation using the results of the retrieval,

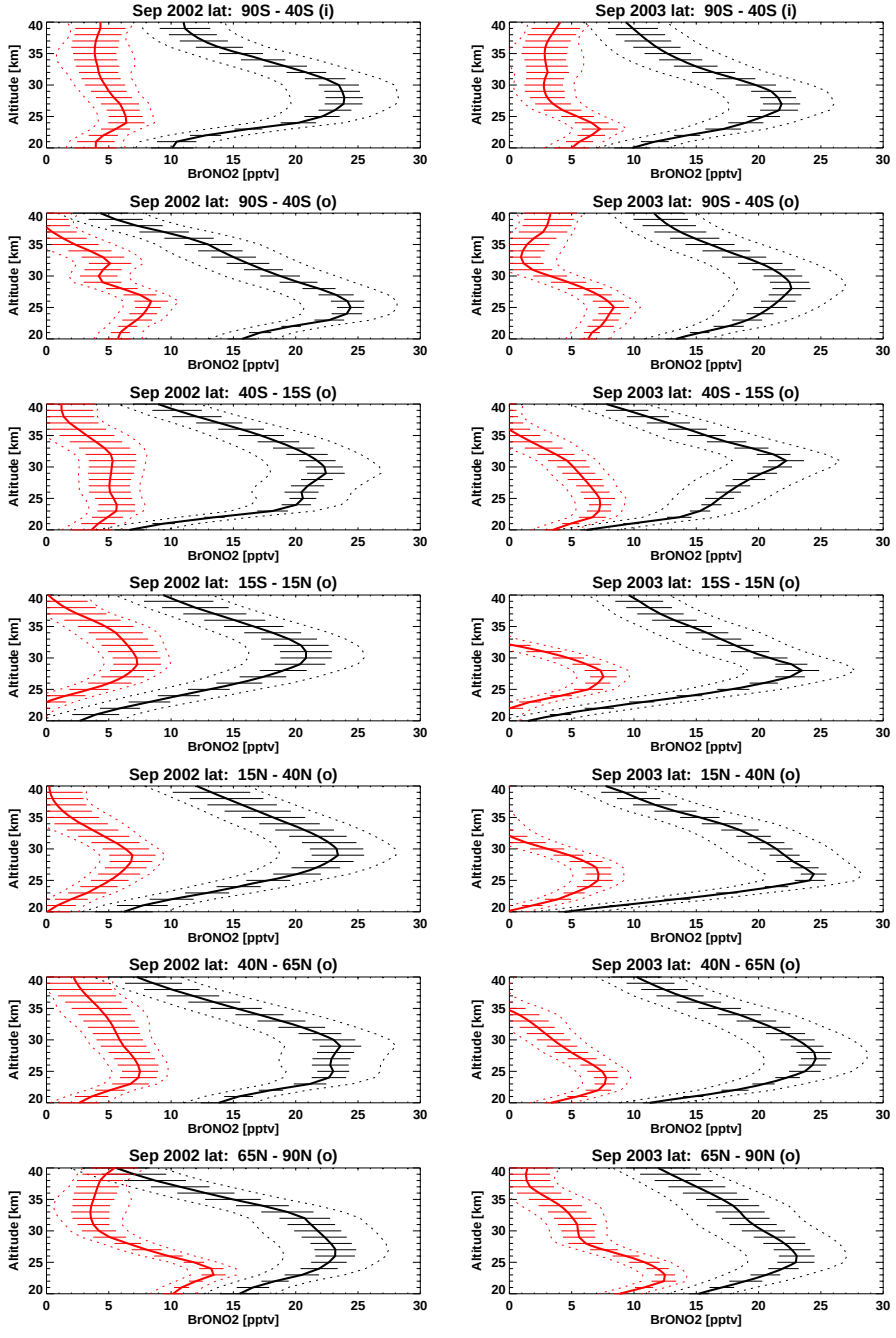

Fig. 2. Retrieved altitude profiles of $BrONO_2$ mixing ratios for September 2002 (left) and 2003 (right) for different latitude ranges and in/out vortex conditions as indicated by (i) and (o) in the title (see Table 1). Red lines indicate daytime while black lines are nighttime observations. Horizontal bars indicate errors due to spectral noise while dotted lines show the range of total uncertainties calculated as the square root of the squared noise errors plus the squared systematic errors described in Sect. 3.4.

$S_{\mathrm{mes}}-S_{\mathrm{sim}}^{\mathrm{all(retAll)}}$) in red are compared with the resulting residual when no $BrONO_2$ but all other gases are fitted ($S_{\mathrm{mes}}-S_{\mathrm{sim}}^{\mathrm{noBr(retnoBr)}}$) in black. Very clearly, for nighttime observations (right column) there remains a residual structure at the position of the $BrONO_2$ ν_3 Q-branch (803–804 cm^{-1}) in the black curve when no $BrONO_2$ has been included in the fit. This residual is totally absent when $BrONO_2$ is included in the retrievals. During daytime, this feature is much smaller indicating low $BrONO_2$ concentrations. The fact that

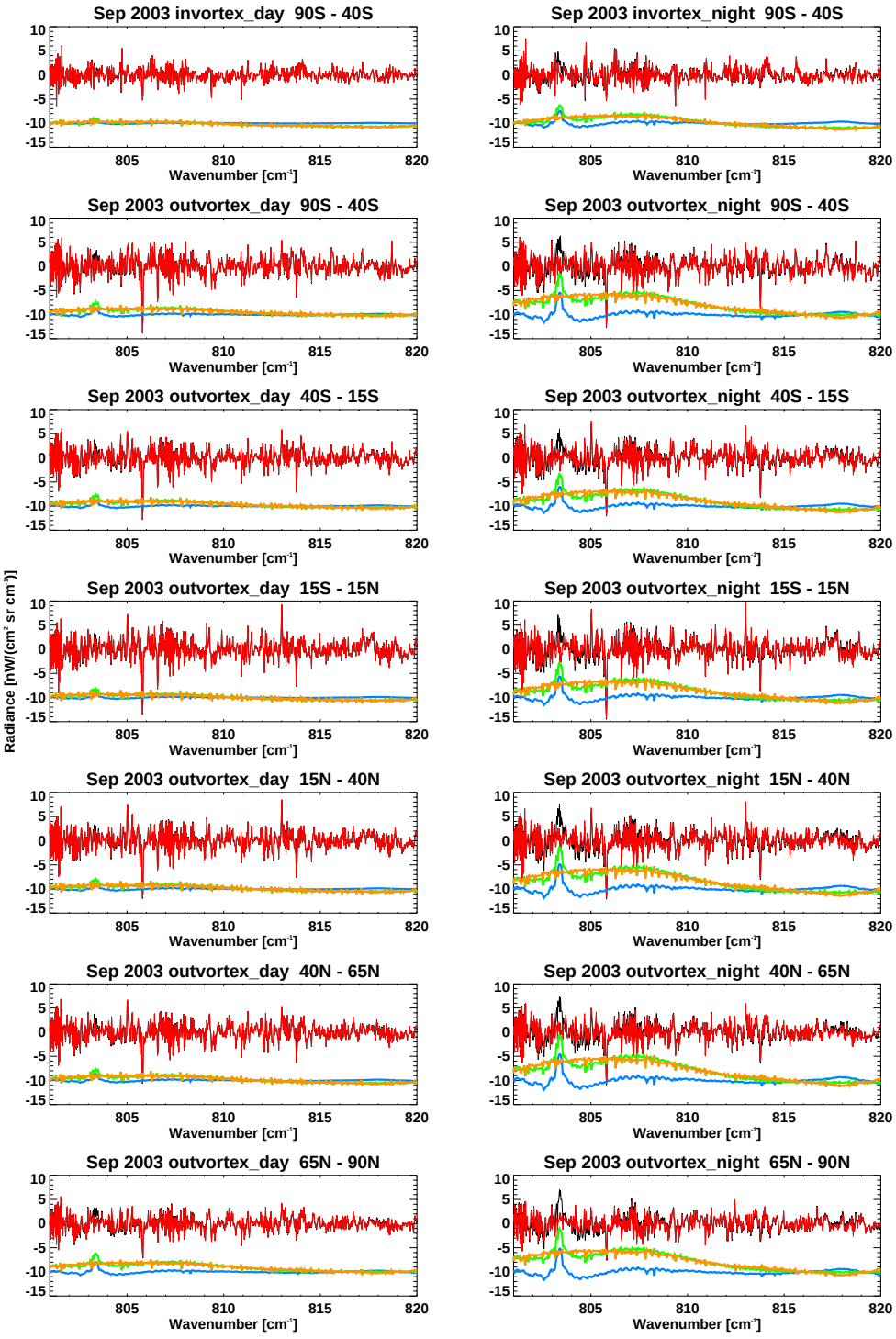

Fig. 3. Residual spectra (measurement-simulation) at around 24 km tangent altitude for retrievals with $BrONO_2$ ($S_{mes} - S_{sim}^{all(retAll)}$: red) and without $BrONO_2$ ($S_{mes} - S_{sim}^{noBr(retnoBr)}$: black) included as a fit-parameter. The left column are daytime while the right column shows nighttime measurements for September 2003. The latitude range and the relative position with respect to the Antarctic polar vortex is given in the title of each plot. Green curves are differences between calculations with-without $BrONO_2$ using profiles of all resulting trace gases from the retrieval including $BrONO_2$ ($S_{sim}^{all(retAll)} - S_{sim}^{noBr(retAll)}$) and the blue curve shows ($S_{sim}^{all(retAll)} - S_{sim}^{noBr(retnoBr)}$). In orange the difference between green and blue ($S_{sim}^{noBr(retnoBr)} - S_{sim}^{noBr(retAll)}$) is shown. For better discrimination, the green, blue and orange curves are all offset by $-10\,nW/(cm^2\,sr\,cm^{-1})$.

the residual is becoming visible, even when a new fit with all known spectrally interfering trace gases except for $BrONO_2$ is performed, clearly proves the detection of $BrONO_2$ by these observations.

Three additional curves in Fig. 3 are plotted to indicate to what extent the spectral feature of $BrONO_2$ can be compensated for by the other trace gases in this spectral region. The green line is the difference of two forward simulations (with and without $BrONO_2$ in the calculations), when all other parameters are fixed to the ones resulting from the original $BrONO_2$ retrieval ($S_{\rm sim}^{\rm all(retAll)} - S_{\rm sim}^{\rm noBr(retAll)}$) while the blue curve is $S_{\rm sim}^{\rm all(retAll)} - S_{\rm sim}^{\rm noBr(retnoBr)}$. The difference between green and blue ($S_{\rm sim}^{\rm noBr(retnoBr)} - S_{\rm sim}^{\rm noBr(retAll)}$) in orange thus shows which feature of the $BrONO_2$-signature (green) can be compensated for by any of the other parameters simultaneously fitted in the retrieval. In the observed region this is mainly the ν_3 *R*-branch. Thus, the unique information about $BrONO_2$ in our measurements stems to a large extend from its *Q*-branch structure.

3.4 Error estimation

3.4.1 Spectroscopic data of $BrONO_2$

Infrared absorption cross-sections of bromine nitrate have been measured first in 1995 (Burkholder et al., 1995) focusing on the ν_3 fundamental band around 803 cm^{-1} and more recently covering also other infrared bands in the 500–2000 cm^{-1} region (Orphal et al., 2008). In particular it is important that the second dataset (that was used as reference absorption cross-sections for the present study) was scaled to the first one using the integrated intensity of the 803 cm^{-1} band (which is the band used here for the infrared retrievals). The infrared measurements by Burkholder et al. were made quasi simultaneously with measurements of the ultraviolet absorption cross-sections of $BrONO_2$ which have also been determined by other authors in the past (Spencer and Rowland, 1978; Deters et al., 1998) and show good agreement.

In order to take into account the variation of the absorption cross-sections of the ν_3 band of $BrONO_2$ as a function of temperature, we have performed a simulation of the temperature effect on the band shape using a standard asymmetric top Hamiltonian based on the rotational constants of $BrONO_2$, estimated from its structural parameters and using the vibrational dependence of the rotational constants determined for $ClONO_2$ (Flaud et al., 2002). The observed temperature variation is very similar to that observed in the ν_2 band of $ClONO_2$ (Orphal et al., 1994), i.e. a narrowing of the band, in particular of the *P*- and *R*-branches, and a sharpening of the *Q*-branch. Using this calculation, the experimental absorption cross-sections at room temperature were scaled to reproduce the modelled effect of the band contour at low temperatures.

The effect of the adaptation of the cross-sections to 218 K is shown in Fig. 4: for most altitudes the resulting vmr values

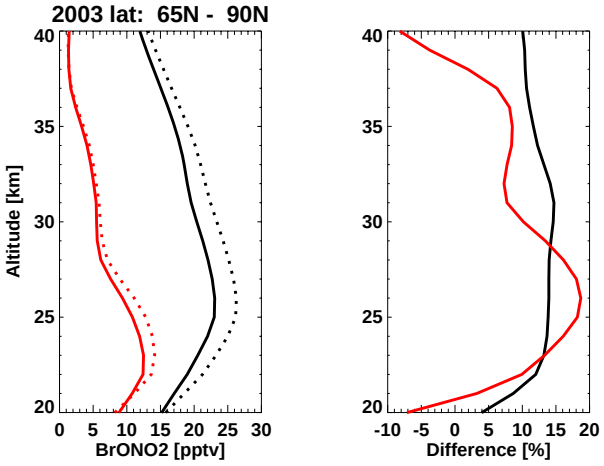

Fig. 4. Comparison of retrievals for latitude range 65–90° N in September 2003 using original $BrONO_2$ cross-sections by Orphal et al. (2008) (dotted) and results for temperature-adjusted cross-sections (solid) as described in Sect. 3.4.1. Daytime observations are in red while nighttime measurements are in black. (Relative differences on the right panel are defined as (dotted-solid)/solid data from the left panel.)

of $BrONO_2$ would have been by about 5–20% higher had the original 296 K cross-sections and not the temperature-scaled ones been used. Although this procedure is less accurate than an experimental determination of the $BrONO_2$ absorption cross-sections at stratospheric temperatures (which is a considerable effort), the systematic error is certainly reduced by this approach.

In addition, another systematic uncertainty is due to the integrated band intensity. In the recent paper by Orphal et al., the integrated band strengths of several fundamental bands of $BrONO_2$ were compared to those of $ClONO_2$ which are also very well established (Goldman et al., 1998; Birk and Wagner, 2003), and significant differences were observed. In particular, from ab-initio calculations (Petkovic, 2007) we expect to observe similar integrated band strengths for both molecules. However, the infrared band strengths of $BrONO_2$ based on the work of Burkholder et al. are systematically lower by about 30% than those of $ClONO_2$. It is therefore possible that the infrared band strengths of $BrONO_2$ as used in this study are too low by up to 30% (thus leading to $BrONO_2$ concentrations that might be up to 30% high). On the other hand, there is very good agreement between three independent measurements of the $BrONO_2$ absorption cross-sections in the ultraviolet-visible region (Spencer and Rowland, 1978; Burkholder et al., 1995; Deters et al., 1998) so that it seems rather unlikely that the infrared band strength of Burkholder et al. (that was determined quasi simultaneously with the ultraviolet-visible cross-sections) is wrong by 30%. New laboratory measurements of the infrared absorption cross-sections of $BrONO_2$ are required to solve this issue

and also to provide accurate reference data at stratospheric temperatures.

For estimation of systematic errors of the retrieval we have assumed an overall 20% uncertainty of the $BrONO_2$ cross-sections comprising the error of the 296 K laboratory dataset and the error of the downscaling to stratospheric temperatures. We have calculated its effect by repeating the retrievals with an 20% scaled cross-section dataset. As indicated by the lines named "spec_Br" in Fig. 5 this results at nearly all altitudes in a 20% bias. Vmrs during daytime are affected by up to nearly 60% only at altitudes above about 33 km.

3.4.2 Retrieval from co-added limb-emission spectra

Due to non-linearity of the radiative transfer, especially in case of mid-infrared emission measurements, retrievals from averaged spectra will generally provide different results than calculating the average profile from single retrievals. Here we treat this effect as an additional error term including uncertainties in the instrumental line-of-sight. To estimate its magnitude we have first simulated as many single MIPAS measurements as those used in the averaging of the real retrieval (Table 1) on basis of (a) ECMWF analyses for pressure and temperature at the original MIPAS locations and times, (b) volume mixing ratio profiles of all interfering trace gases randomly disturbed by their climatological standard deviation (Remedios et al., 2007), (c) the originally resulting $BrONO_2$ profiles as in Fig. 2 disturbed with a standard deviation of 50%, and (d) a line-of-sight uncertainty of 150 m at the tangent points (von Clarmann et al., 2003). The simulated single spectra have been averaged and retrievals have then been performed in the same way as has been done with the original MIPAS observations. Errors have been estimated as mean differences between the retrieved and the "true" mean profile of $BrONO_2$ separately for day and nighttime observations and are shown in Fig. 5 indicated as "nlin": over the whole altitude range during night and below 30 km during day errors range between 0.1 and 1.3 pptv (1–10%) while above 30 km during day errors up to 2 pptv (120%) are reached.

3.4.3 Interfering species and instrumental line-shape

The influence of errors due to the spectroscopy of the major interfering species CO_2, O_3 and H_2O has been estimated by perturbing (a) the line intensities by 5% and, (b) the pressure-broadening half-widths by 10% and, on basis of those, performing new retrievals. Resulting differences are in case of line-intensity around 1–3% (0.1–0.2 pptv) which is smaller than the assumed intensity errors due to compensational effects with the trace gas concentrations and temperature ("spec_int" in Fig. 5). Half-width induced errors range between 5 and 20% (0.5–2.2 pptv) for all altitudes during night and below 30 km during day while above 30 km during day maximum errors reach 80% ("spec_hw" in Fig. 5).

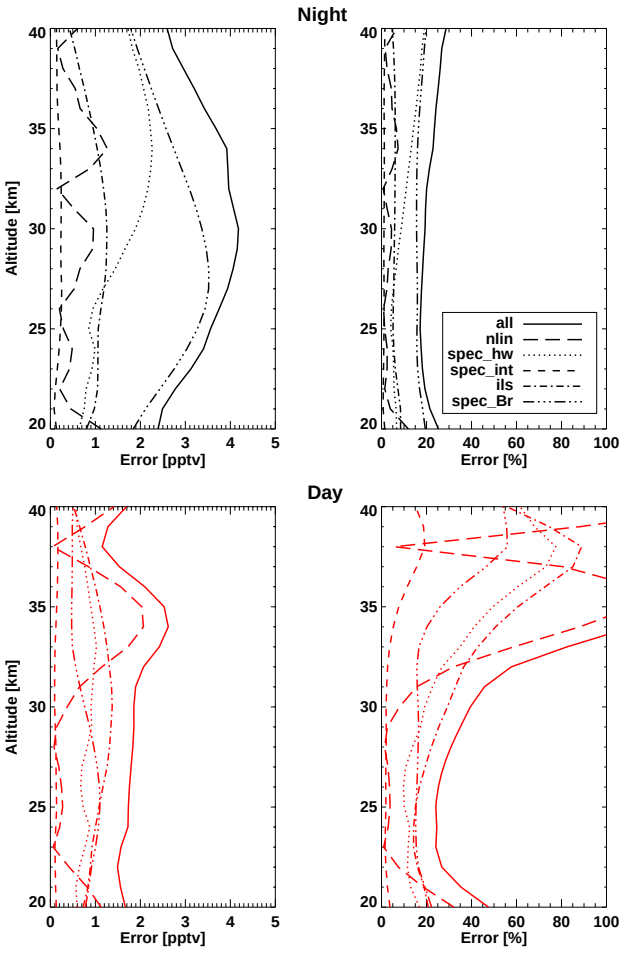

Fig. 5. Budget of systematic errors for mean day and nighttime profiles of $BrONO_2$. Errors due to retrieval from mean radiance spectra: nlin; due to uncertainties in the spectroscopic data (line half-width and intensity) of the major interfering species O_3, CO_2 and H_2O: spec_hw and spec_int; due to knowledge of the in the instrumental line shape of MIPAS: ils; and due to the spectroscopy of $BrONO_2$: spec_Br. The Gaussian combination of all errors is indicated by the solid lines.

The knowledge of the instrumental line shape, which has been estimated to within 3% (F. Hase, personal communication; Höpfner et al., 2007), is a further parameter influencing the quality of the fit between simulated and observed mean spectra. Resulting errors range from 0.5 to 1.4 pptv and are indicated as "ils" in Fig. 5.

4 Comparison with a photochemical model

Using a simple photochemical model, daytime $BrONO_2$ concentrations have been calculated for the various latitude bands as

$$[BrONO_2]=\frac{k_1[NO_2][BrO]}{j_1+j_2} \quad \text{(R1)}$$

where k_1 is the reaction rate of the termolecular reaction (Thorn et al., 1993)

$$k_1 : BrO + NO_2 + M \rightarrow BrONO_2 + M \quad \text{(R2)}$$

and its value was determined using the rate constants recommended by Sander et al. (2006). The photolysis frequencies

$$j_1 : BrONO_2 + h\nu \rightarrow BrO + NO_2 \quad \text{(R3)}$$

$$j_2 : BrONO_2 + h\nu \rightarrow Br + NO_3 \quad \text{(R4)}$$

were calculated with the interactive TUV model version 4.4 (Madronich and Flocke, 1998), (http://cprm.acd.ucar.edu/Models/TUV/Interactive_TUV). The NO_2 concentrations were obtained from the NO_2 volume mixing ratios of the related latitude band retrieved directly from the MIPAS spectra along with $BrONO_2$. The BrO concentrations were taken from the paper by Sinnhuber et al. (2005) who reported observations during September 2002 by the SCIAMACHY instrument, that is also installed aboard the Envisat satellite and performs stratospheric BrO measurements in limb geometry. In addition to this baseline "model 1" runs, in "model 2" we included the reaction $BrONO_2$+O(^{3}P) (Soller et al., 2001) using O(^{3}P) concentration profiles from the model by Garcia (1983).

The modelled $BrONO_2$ concentrations based on observed NO_2 and BrO vmr profiles are compared to the MIPAS daytime measurements in Fig. 6. We have restricted these comparisons to latitudes north of 40° S in order to avoid polar vortex airmasses influenced by heterogeneous chemistry at polar stratospheric clouds. The measured and modelled $BrONO_2$ concentrations agree well within the estimated uncertainty range in most cases. Only in the latitude region 65–90° N the modelled $BrONO_2$ concentrations at altitudes of 21–24 km are in case of "model 1" clearly and with "model 2" still slightly overestimated. In general, however, it is difficult to decide whether "model 1" or "model 2" obtains better results: while "model 2" agrees better with the observations within the latitude bin 65–90° N "model 1" fits better in the rest of the latitude ranges.

A potential sink for $BrONO_2$ not considered by the equilibrium calculations could be the hydrolysis of $BrONO_2$ at stratospheric background aerosol. Lary et al. (1996) estimated the influence on the $BrONO_2/BrO_y$ diurnal cycle at 37.9° N, 66.9 hPa for an aerosol surface area density of 6 $\mu m^2\,cm^{-3}$. Around noon this resulted in a reduction of $BrONO_2$ by about 25%. However, this aerosol surface area is

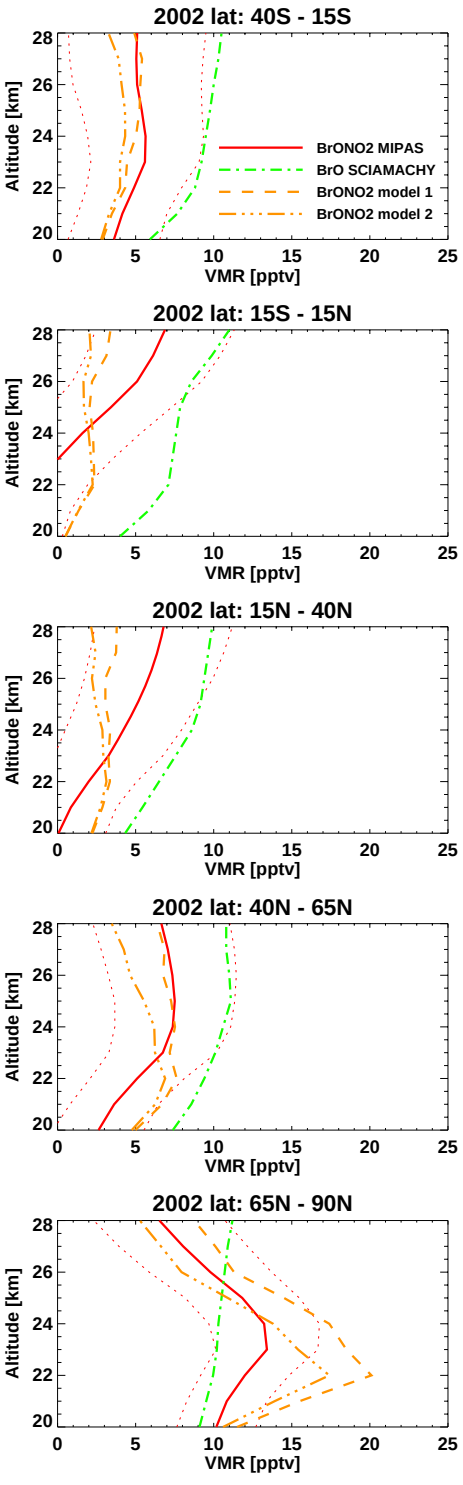

Fig. 6. Comparison between MIPAS daytime measurements of $BrONO_2$ outside the polar vortex for September 2002 and photochemical equilibrium model results for $BrONO_2$ ("model 1": without, "model 2": with reaction $BrONO_2$ + O(^{3}P) (Soller et al., 2001)) based on SCIAMACHY BrO observations during the same month (Sinnhuber et al., 2005).

valid for enhanced volcanic situations while background levels in 2002 were about a factor of 10 lower (e.g. Thomason and Peter, 2006). Thus, the effect on our comparison would be a reduction of the modelled $BrONO_2$ of only a few percent, which is too low to explain the overestimated values at lower altitudes.

The consistency of the infrared and the ultraviolet absorption cross-sections of $BrONO_2$ employed here is an important point when comparing the observed $BrONO_2$ concentrations with the predictions of the photochemical model: any systematic bias of the infrared cross-sections would also be present in the ultraviolet absorption cross-sections, leading to a rather robust comparison (i.e. insensitive of the absolute cross-section values). For example, higher infrared absorption cross-sections will not only lead to smaller $BrONO_2$ concentrations retrieved from the infrared spectra, but also to higher $BrONO_2$ photolysis rates (through the higher ultraviolet absorption cross-sections), so that the $BrONO_2$ concentrations predicted from the photochemical model would also be smaller. Therefore the most important issue for the comparison of observed $BrONO_2$ concentrations with those predicted from a photochemical model (and based on the observed BrO concentrations) is the consistency of the infrared and the ultraviolet absorption cross-sections of $BrONO_2$, which has been established by the laboratory measurements of Burkholder et al. (1995).

These calculations confirm the general consistency of the measured $BrONO_2$ concentration profiles from MIPAS and of the BrO concentrations from SCIAMACHY mostly within the estimated measurement errors. It will be important in the future to improve the accuracy of the measured $BrONO_2$ concentrations for a more quantitative analysis of simultaneous measurements of $BrONO_2$, BrO and NO_2.

5 Conclusions

We have presented the first measurements of stratospheric $BrONO_2$ and its global distribution. From the analysis presented above it is evident that stratospheric $BrONO_2$ can be detected using infrared spectroscopy. The MIPAS spectra have been carefully calibrated and the methodology for data analysis has been successfully applied to many other atmospheric trace species in the past. In particular, inspection of the spectral residuals clearly shows the presence of $BrONO_2$ in the MIPAS spectra. It is therefore expected that other infrared experiments (including spectra recorded with balloon-borne and ground-based instruments, and also using solar occultation) will provide $BrONO_2$ concentrations in the future.

The following observations can be made using the first measurements of stratospheric $BrONO_2$ profiles presented here. First, as expected from photochemical models of stratospheric bromine chemistry, there is a very clear diurnal variation of the $BrONO_2$ concentrations, with much higher concentrations during the night, and this clearly confirms the predicted behaviour of stratospheric $BrONO_2$ as bromine reservoir. Second, the night-time $BrONO_2$ mixing ratio profiles show a maximum in the 25–31 km region, which is again in good agreement with photochemical models, although the maximum seems to be slightly broader (which can be partly due to the limited vertical resolution of the MIPAS observations). The daytime profiles show different structure and a clear latitudinal dependence of the maximum. Third, the observed $BrONO_2$ vertical profiles are rather similar for 2002 and 2003. Maximum values of the $BrONO_2$ volume mixing ratios during night are always in the range 20–25 pptv which is in agreement with estimates of total inorganic stratospheric bromine of 18–25 pptv (WMO, 2007). Finally, first comparisons of MIPAS daytime $BrONO_2$ profiles with photochemical equilibrium calculations based on SCIAMACHY BrO observations show reasonable agreement within the estimated errors.

MIPAS measurements of stratospheric $BrONO_2$ volume mixing ratios are in good general agreement with the currently established picture of stratospheric bromine chemistry concerning the total amount of inorganic bromine and the partitioning of stratospheric bromine, including the diurnal variation of $BrONO_2$. Future work will focus on the detailed quantitative analysis of the MIPAS data. New laboratory measurements of $BrONO_2$ to reduce the systematic errors will be carried out. It is also expected that detailed analysis of simultaneous observations of other species – in particular BrO and NO_2 – will provide additional insight into stratospheric bromine chemistry.

Acknowledgements. The authors wish to thank C. Keim (LISA, Université de Paris-Est, Créteil, France) for helpful discussions and S. Madronich (NCAR, Boulder, USA) for maintenance of and advice with respect to the interactive TUV model.

Edited by: M. Dameris

References

Aliwell, S. R., Jones, R. L., and Fish, D. J.: Mid-latitude observations of the seasonal variation of BrO. 1. Zenith-sky measurements, Geophys. Res. Lett., 24, 1195–1198, 1997.

Avallone, L. M. and Toohey, D. W.: Tests of halogen photochemistry using in situ measurements of ClO and BrO in the lower polar stratosphere, J. Geophys. Res. D, 106, 10411–10421, 2001.

Birk, M. and Wagner, G.: New infrared spectroscopic database for chlorine nitrate, J. Quant. Spectrosc. Rad. Transf., 82, 443–460, 2003.

Burkholder, J. B., Ravishankara, A. R., and Solomon, S.: UV/Visible and IR absorption cross sections of $BrONO_2$, J. Geophys. Res. D, 100, 16793–16800, 1995.

Carlotti, M., Ade, P. A. R., Carli, B., Ciarpallini, P., Cortesi, U., Griffin, M. J., Lepri, G., Mencaraglia, F., Murray, A. G., Nolt, I. G., Park, J. H., and Radostitz, J. V.: Measurement of stratospheric HBr using high resolution far infrared spectroscopy, Geophys. Res. Lett., 22, 3207–3210, 1995.

Daniel, J. S., Solomon, S., Portmann, R. W., and Garcia, R. R.: Stratospheric ozone destruction: The importance of bromine relative to chlorine, J. Geophys. Res. D, 104, 23871–23880, 1999.

Deters, B., Burrows, J. P., and Orphal, J.: UV-visible absorption cross-sections of bromine nitrate determined by photolysis of $BrONO_2/Br_2$ mixtures, J. Geophys. Res. D, 103, 3536–3570, 1998.

Dorf, M., Butler, J. H., Butz, A., Camy-Peyret, C., Chipperfield, M. P., Kritten, L., Montzka, S. A., Simmes, B., Weidner, F., and Pfeilsticker, K.: Long-term observations of stratospheric bromine reveal slow down in growth, Geophys. Res. Lett., 33, L24803, doi:10.1029/2006GL027714, 2006.

Fischer, H., Birk, M., Blom, C., Carli, B., Carlotti, M., von Clarmann, T., Delbouille, L., Dudhia, A., Ehhalt, D., Endemann, M., Flaud, J. M., Gessner, R., Kleinert, A., Koopman, R., Langen, J., López-Puertas, M., Mosner, P., Nett, H., Oelhaf, H., Perron, G., Remedios, J., Ridolfi, M., Stiller, G., and Zander, R.: MIPAS: an instrument for atmospheric and climate research, Atmos. Chem. Phys., 8, 2151–2188, 2008, http://www.atmos-chem-phys.net/8/2151/2008/.

Fish, D. J., Jones, R. L., and Strong, E. K.: Midlatitude observations of the diurnal variation of stratospheric BrO, J. Geophys. Res. D, 100, 18863–18871, 1995.

Fish, D. J., Aliwell, S. R., and Jones, R. L.: Mid-latitude observations of the seasonal variation of BrO. 2. Interpretation and modelling study, Geophys. Res. Lett., 24, 1199–1202, 1997.

Flaud, J.-M., Orphal, J., Lafferty, W. J., Birk, M., and Wagner, G.: High-resolution vib-rotational analysis of the ν_3 and ν_4 spectral regions of chlorine nitrate, J. Geophys. Res., 107, 4782, doi:10.1029/2002JD002628, 2002.

Garcia, R. R.: A numerical model of the zonally averaged dynamical and chemical structure of the middle atmosphere, J. Geophys. Res., 88, 1379–1400, 1983.

Goldman, A., Rinsland, C. P., Flaud, J.-M., and Orphal, J.: $ClONO_2$: spectroscopic line parameters and cross-sections in 1996 HITRAN, J. Quant. Spectrosc. Rad. Transf., 60, 875–882, 1998.

Hanson, D. R., Ravishankara, A. R., and Lovejoy, E. R.: Reaction of $BrONO_2$ with H_2O on submicron sulfuric acid aerosol and the implications for the lower stratosphere, J. Geophys. Res. D, 101, 9063–9069, 1996.

Harder, H., Bösch, H., Camy-Peyret, C., Chipperfield, M. P., Fitzenberger, R., Payan, S., Perner, D., Platt, U., Sinnhuber, B.-M., and Pfeilsticker, K.: Comparison of measured and modeled stratospheric BrO: Implications for the total amount of stratospheric bromine, Geophys. Res. Lett., 27, 3695–3698, 2000.

Hendrick, F., Johnston, P. V., De Maziere, M., Fayt, C., Hermans, C., Kreher, K., Theys, N., Thomas, A., and Van Roozendael, M.: One-decade trend analysis of stratospheric BrO over Harestua (60°N) and Lauder (45°S) reveals a decline, Geophys. Res. Lett., 35, L14801, doi:10.1029/2008GL034154, 2008.

Höpfner, M., von Clarmann, T., Fischer, H., Funke, B., Glatthor, N., Grabowski, U., Kellmann, S., Kiefer, M., Linden, A., Milz, M., Steck, T., Stiller, G. P., Bernath, P., Blom, C. E., Blumenstock, Th., Boone, C., Chance, K., Coffey, M. T., Friedl-Vallon, F., Griffith, D., Hannigan, J. W., Hase, F., Jones, N., Jucks, K. W., Keim, C., Kleinert, A., Kouker, W., Liu, G. Y., Mahieu, E., Mellqvist, J., Mikuteit, S., Notholt, J., Oelhaf, H., Piesch, C., Reddmann, T., Ruhnke, R., Schneider, M., Strandberg, A., Toon, G., Walker, K. A., Warneke, T., Wetzel, G., Wood, S., and Zander, R.: Validation of MIPAS $ClONO_2$ measurements, Atmos. Chem. Phys., 7, 257–281, 2007, http://www.atmos-chem-phys.net/7/257/2007/.

Johnson, D. G., Traub, W. A., Chance, K. V., and Jucks, K. W.: Detection of HBr and upper limit of HOBr: Bromine partitioning in the stratosphere, Geophys. Res. Lett., 22, 1373–1376, 1995.

Johnson, D. G., Orphal, J., Toon, G. C., Chance, K. V., Traub, W. A., Jucks, K. W., Guelachvili, G., and Morillon-Chapey, M.: Measurement of chlorine nitrate in the stratosphere using the ν_4 and ν_5 bands, Geophys. Res. Lett., 23, 1745–1748, 1996.

Kovalenko, L. J., Livesey, N. L., Salawitch, R. J., Camy-Peyret, C., Chipperfield, M. P., Cofield, R. E., Dorf, M., Drouin, B. J., Froidevaux, L., Fuller, R. A., Goutail, F., Jarnot, R. F., Jucks, K., Knosp, B. W., Lambert, A., MacKenzie, I. A., Pfeilsticker, K., Pommereau, J.-P., Read, W. G., Santee, M. L., Schwartz, M. J., Snyder, W. V., Stachnik, R., Stek, P. C., Wagner, P. A., and Waters, J. W.: Validation of Aura Microwave Limb Sounder BrO observations in the stratosphere, J. Geophys. Res. D, 112, D24S41, doi:10.1029/2007JD008817, 2007.

Lary, D. J.: Gas phase atmospheric bromine photochemistry, J. Geophys. Res. D, 101, 1505–1516, 1996.

Lary, D. J., Chipperfield, M. P., Toumi, R., and Lenton, T.: Heterogeneous atmospheric bromine chemistry, J. Geophys. Res. D, 101, 1489–1504, 1996.

Madronich, S. and Flocke, S.: The role of solar radiation in atmospheric chemistry, in: Handbook of Environmental Chemistry, edited by: Boule, P., Springer-Verlag, Heidelberg, 1–26, 1998.

Nett, H., Carli, B., Carlotti, M., Dudhia, A., Fischer, H., Flaud, J.-M., Perron, G., Raspollini, P., and Ridolfi, M.: MIPAS Ground Processor and Data Products, in: Proc. IEEE 1999 International Geoscience and Remote Sensing Symposium, 28 June–2 July 1999, Hamburg, Germany, 1692–1696, 1999.

Nolt, I. G., Ade, P. A. R., Alboni, F., Carli, B., Carlotti, M., Cortesi, U., Epifani, M., Griffin, M. J., Hamilton, P. A., Lee, C., Lepri, G., Mencaraglia, F., Murray, A. G., Park, J. H., Park, K., Raspollini, P., Ridolfi, M., and Vanek, M. D.: Stratospheric HBr concentration profile obtained from far-infrared emission spectroscopy, Geophys. Res. Lett., 24, 281–284, 1997.

Norton, H. and Beer, R.: New apodizing functions for Fourier spectrometry, J. Opt. Soc. Am., 66, 259–264, (Errata J. Opt. Soc. Am., 67, p. 419, 1977), 1976.

Orphal, J., Morillon-Chapey, M., and Guelachvili, G.: High-resolution absorption cross sections of chlorine nitrate in the ν_2 band region around 1292 cm^{-1} at stratospheric temperatures, J. Geophys. Res. D, 99, 14549–14555, 1994.

Orphal, J., Morillon-Chapey, M., and Guelachvili, G.: Infrared band intensities of bromine nitrate, $BrONO_2$, Chem. Phys. Lett., 458, 44–47, 2008.

Petkovic, M.: Infrared spectroscopy of $ClONO_2$ and $BrONO_2$ investigated by means of anharmonic force fields, Chem. Phys., 331, 438–446, 2007.

Pfeilsticker, K., Sturges, W., Bosch, H., Camy-Peyret, C., Chipperfield, M., Engel, A., Fitzenberger, R., Muller, M., Payan, S., and Sinnhuber, B.: Lower stratospheric organic and inorganic bromine budget for the Arctic winter 1998/99, Geophys. Res. Lett., 27, 3305–3308, 2000.

Pundt, I., Pommereau, J.-P., Chipperfield, M. P., Van Roozendael, M., and Goutail, F.: Climatology of the stratospheric BrO ver-

tical distribution by balloon-borne UV-visible spectrometry, J. Geophys. Res. D, 107, 4806, doi:10.1029/2002JD002230, 2002.

Remedios, J. J., Leigh, R. J., Waterfall, A. M., Moore, D. P., Sembhi, H., Parkes, I., Greenhough, J., Chipperfield, M.P., and Hauglustaine, D.: MIPAS reference atmospheres and comparisons to V4.61/V4.62 MIPAS level 2 geophysical data sets, Atmos. Chem. Phys. Discuss., 7, 9973–10017, 2007, http://www.atmos-chem-phys-discuss.net/7/9973/2007/.

Rodgers, C. D.: Inverse Methods for Atmospheric Sounding: Theory and Practice, Vol. 2, Series on Atmospheric, Oceanic and Planetary Physics, edited by: Taylor, F. W., World Scientific, 2000.

Salawitch, R. J., Weisenstein, D. K., Kovalenko, L. J., Sioris, C. E., Wennberg, P. O., Chance, K. V., Ko, M. K. W., and McLinden, C. A.: Sensitivity of ozone to bromine in the lower stratosphere, Geophys. Res. Lett., 32, L05811, doi:10.1029/2004GL021504, 2005.

Sander, S. P., Golden, D. M., Kurylo, M. J., Moortgat, G. K., Wine, P. H., Ravishankara, A. R., Kolb, C. E., Molina, M. J., Finlayson-Pitts, B. J., Huie, R. E., Orkin, V. L., Friedl, R. R., and Keller-Rudek, H.: Chemical kinetics and photochemical data for use in atmospheric studies: evaluation number 15, JPL Publication 06-2, Jet Propulsion Laboratory, California Institute of Technology, Pasadena, CA, 2006.

Sheode, N., Sinnhuber, B.-M., Rozanov, A., and Burrows, J. P.: Towards a climatology of stratospheric bromine monoxide from SCIAMACHY limb observations, Atmos. Chem. Phys. Discuss., 6, 6431–6466, 2006, http://www.atmos-chem-phys-discuss.net/6/6431/2006/.

Sinnhuber, B.-M., Arlander, D. W., Bovensmann, H., Burrows, J. P., Chipperfield, M. P., Enell, C. F., Friess, U., Hendrick, F., Johnston, P. V., Jones, R. L., Kreher, K., Mohamed-Tahrin, N., Muller, R., Pfeilsticker, K., Platt, U., Pommereau, J.-P., Pundt, I., Richter, A., South, A. M., Tornkvist, K. K., Van Roozendael, M., Wagner, T., and Wittrock, F.: Comparison of measurements and model calculations of stratospheric bromine monoxide, J. Geophys. Res. D, 107, 4398, doi:10.1029/2001JD000940, 2002.

Sinnhuber, B.-M., Rozanov, A., Sheode, N., Afe, O. T., Richter, A., Sinnhuber, M., Wittrock, F., Burrows, J. P., Stiller, G. P., von Clarmann, T., and Linden, A.: Global observations of stratospheric bromine monoxide from SCIAMACHY, Geophys. Res. Lett., 32, L20810, doi:10.1029/2005GL023839, 2005.

Sioris, C. E., Kovalenko, L. J., McLinden, C. A., Salawitch, R. J., Van Roozendael, M., Goutail, F., Dorf, M., Pfeilsticker, K., Chance, K., von Savigny, C., Liu, X., Kurosu, T. P., Pommereau, J. P., Boesch, H., and Frerick, J.: Latitudinal and vertical distribution of bromine monoxide in the lower stratosphere from Scanning Imaging Absorption Spectrometer for Atmospheric Chartography limb scattering measurements, J. Geophys. Res. D, 111, D14301, doi:10.1029/2005JD006479, 2006.

Soller, R., Nicovich, J., and Wine, P.: Temperature-dependent rate coefficients for the reactions of $Br(^2P_{3/2})$, $Cl(^2P_{3/2})$, and $O(^3P)$ with $BrONO_2$, J. Phys. Chem. A, 105, 1416–1422, 2001.

Soller, R., Nicovich, J. M., and Wine, P. H.: Bromine nitrate photochemistry: Quantum yields for O, Br, and BrO over the wavelength range 248-355 nm, J. Phys. Chem. A, 106, 8378–8385, doi:10.1021/jp020018r, 2002.

Spang, R., Remedios, J. J., and Barkley, M. P.: Colour indices for the detection and differentiation of cloud types in infra-red limb emission spectra, Adv. Space Res., 33, 1041–1047, 2004.

Spencer, J. E. and Rowland, F. S.: Bromine nitrate and its stratospheric significance, J. Phys. Chem., 82, 7–10, 1978.

Stiller, G. P. (Ed.): The Karlsruhe Optimized and Precise Radiative Transfer Algorithm (KOPRA), Vol. FZKA 6487, Wissenschaftliche Berichte, Forschungszentrum Karlsruhe, 2000.

Stiller, G. P., von Clarmann, T., Höpfner, M., Glatthor, N., Grabowski, U., Kellmann, S., Kleinert, A., Linden, A., Milz, M., Reddmann, T., Steck, T., Fischer, H., Funke, B., López-Puertas, M., and Engel, A.: Global distribution of mean age of stratospheric air from MIPAS SF6 measurements, Atmos. Chem. Phys., 8, 677–695, 2008, http://www.atmos-chem-phys.net/8/677/2008/.

Thomason, L. and Peter, T.: Assessment of Stratospheric Aerosol Properties (ASAP), Tech. Rep. 4, Stratospheric Processes and their Role in Climate, SPARC, 2006.

Thorn, R. P., Daykin, E., and Wine, P.: Kinetics of the BrO + NO_2 association reaction. Temperature and pressure dependence in the falloff regime, Int. J. Chem. Kinet., 25, 521–537, 1993.

Tie, X. X. and Brasseur, G.: The importance of heterogeneous bromine chemistry in the lower stratosphere, Geophys. Res. Lett., 23, 2505–2508, 1996.

Tikhonov, A.: On the solution of incorrectly stated problems and method of regularization, Dokl. Akad. Nauk. SSSR, 151, 501–504, 1963.

von Clarmann, T., Glatthor, N., Grabowski, U., Höpfner, M., Kellmann, S., Kiefer, M., Linden, A., Mengistu Tsidu, G., Milz, M., Steck, T., Stiller, G. P., Wang, D. Y., Fischer, H., Funke, B., Gil-López, S., and López-Puertas, M.: Retrieval of temperature and tangent altitude pointing from limb emission spectra recorded from space by the Michelson Interferometer for Passive Atmospheric Sounding (MIPAS), J. Geophys. Res., 108, 4736, doi:10.1029/2003JD003602, 2003.

WMO: Scientific assessment of ozone depletion: 2006, Global Ozone Research and Monitoring Project, Report No. 50, World Meteorological Organization, 2007.